# A novel truncated form of apolipoprotein A-I transported by dense LDL is increased in diabetic patients[1] [S]

**Judit Cubedo,* Teresa Padró,* Maisa García-Arguinzonis,* Gemma Vilahur,* Inka Miñambres,† Jose María Pou,† Juan Ybarra,§ and Lina Badimon[2,*,**]**

Cardiovascular Research Center (CSIC-ICCC),* Biomedical Research Institute Sant Pau (IIB-Sant Pau), Barcelona, Spain; Endocrinology Department,† Hospital de la Santa Creu i Sant Pau, Barcelona, Spain; Teknon Medical Center,§ Barcelona, Spain; and Cardiovascular Research Chair,** Universitat Autònoma de Barcelona, Barcelona, Spain

**Abstract Diabetic (DM) patients have exacerbated atherosclerosis and high CVD burden. Changes in lipid metabolism, lipoprotein structure, and dysfunctional HDL are characteristics of diabetes. Our aim was to investigate whether serum ApoA-I, the main protein in HDL, was biochemically modified in DM patients. By using proteomic technologies, we have identified a 26 kDa ApoA-I form in serum. MS analysis revealed this 26 kDa form as a novel truncated variant lacking amino acids 1-38, ApoA-IΔ(1-38). DM patients show a 2-fold increase in ApoA-IΔ(1-38) over nondiabetic individuals. ApoA-IΔ(1-38) is found in LDL, but not in VLDL or HDL, with an increase in LDL3 and LDL4 subfractions. To identify candidate mechanisms of ApoA-I truncation, we investigated potentially involved enzymes by in silico data mining, and tested the most probable molecule in an established animal model of diabetes. We have found increased hepatic cathepsin D activity as one of the potential proteases involved in ApoA-I truncation. Cathepsin D-cleaved ApoA-I exhibited increased LDL binding affinity and decreased antioxidant activity against LDL oxidation. In conclusion, we show for the first time: *a*) presence of a novel truncated ApoA-I form, ApoA-IΔ(1-38), in human serum; *b*) ApoA-IΔ(1-38) is transported by LDL; *c*) ApoA-IΔ(1-38) is increased in dense LDL fractions of DM patients; and *d*) cathepsin D-ApoA-I truncation may lead to ApoA-IΔ(1-38) binding to LDLs, increasing their susceptibility to oxidation and contributing to the high cardiovascular risk of DM patients.—**Cubedo, J., T. Padró, M. García-Arguinzonis, G. Vilahur, I. Miñambres, J. M. Pou, J. Ybarra, and L. Badimon. **A novel truncated form of apolipoprotein A-I transported by dense LDL is increased in diabetic patients. *J. Lipid Res.* 2015.** 56: **1762–1773.**

**Supplementary key words** diabetes • hyperglycemia • low density lipoprotein • proteomics

Atherosclerotic CVD is the main cause of death in diabetic (DM) patients (1). Indeed, patients with diabetes show two to three times higher coronary risk than nondiabetic (nonDM) patients (2). Several large clinical trials have demonstrated the importance of plasma lipoproteins in the pathogenesis of coronary artery disease (CAD) (3). It is well-known that high levels of LDLs are considered to be a key contributor to the initiation and progression of atherosclerosis (4), and are, therefore, one of the strongest predictors of CAD in both DM and nonDM patients (5). In contrast, elevated levels of HDLs strongly correlate with reduced cardiovascular risk (6). The structure and cholesterol transport ability of HDL particles are determined by the properties of their exchangeable apolipoprotein components (7). ApoA-I is the main protein in HDLs, representing 70% of its total protein content, and is central to HDL assembly, remodeling, and metabolism (8). In addition to its structural role, ApoA-I has a functional role in reverse cholesterol transport by promoting the efflux of cholesterol from peripheral cells into HDLs and activating LCAT (9). During reverse cholesterol transport, ApoA-I transitions from lipid-free protein to spherical HDL particles through a particle remodeling process (10). First, lipid-free/lipid-poor ApoA-I acquires phospholipid and cholesterol through ABCA1 (11) and generates

*This work was supported by grants from the Spanish Ministry of Economy and Competitiveness of Science (SAF2013-42962-R to L.B. and SAF2012-40208 to G.V.) and Institute of Health Carlos III, ISCIII (TERCEL RD12/0019/0026 and RIC RD12/0042/0027 to L.B. and PI13/02850 to T.P.). The authors declare no financial conflicts of interest.*

*Manuscript received 8 January 2015 and in revised form 22 June 2015.*

*Published, JLR Papers in Press, July 13, 2015*
*DOI 10.1194/jlr.P057513*

Abbreviations: aa, amino acid; AGE, advanced glycation end product; CAD, coronary artery disease; CE, cholesteryl ester; 1-DE, one-dimensional gel electrophoresis; 2-DE, two-dimensional gel electrophoresis; DM, diabetic; FC, free cholesterol; LPC, lysophosphatidylcholine; LPDS, lipoprotein-depleted serum; LPE, lysophosphatidylethanolamine; LPS, lysophosphatidylserine; PC, phosphatidylcholine; PE, phosphatidylethanolamine; PS, phosphatidylserine; TRAP, total peroxyl radical-trapping antioxidant potential.

[1] Parts of this study were presented in abstract form at the Congress of the European Society of Cardiology, Munich, Germany, August 25–29, 2012 and published in the European Heart Journal 2012; 33 Abstract Supplement: 280; and at the Congress of the Spanish Society of Cardiology, Valencia, Spain, October 24–26, 2013 and published in Revista Española de Cardiología, 2013; 66 (Suppl. 1): 356.

[2] To whom correspondence should be addressed.
e-mail: lbadimon@csic-iccc.org

[S] The online version of this article (available at http://www.jlr.org) contains a supplement.

nascent HDLs. Second, cholesterol on nascent HDL is esterified by LCAT to yield cholesteryl ester (CE) (12) and mature spherical HDLs. In pioneering studies, we reported that homologous VHDLs (HDL3, VHDL rich in ApoA-I) injections in rabbits, without modifying HDL-cholesterol plasma levels, delayed atherosclerotic plaque formation and induced atherosclerotic plaque regression (13). Years later, this effect was shown in humans treated with ApoA-I Milano (14). ApoA-I is also responsible for the recognition of HDLs by liver SRB1 receptors (15). Among all apolipoproteins, levels of ApoA-I correlate with the protective effect of HDLs against atherosclerosis (16).

ApoA-I is initially synthesized as a prepro-apolipoprotein of 267 amino acids (aas), and it is secreted in an immature form after the removal of the signal peptide (first 18 aas) that is named pro-ApoA-I (aas 19-267). Finally, during its maturation process the pro-peptide is removed, resulting in the mature form of ApoA-I of 243 aas and a molecular mass of 28 kDa (aas 25-267) (17). Besides some posttranslational modifications during processing, abnormal circulating ApoA-I variants have also been identified. Recently, a C-terminal truncated form that expressed with reduced cholesterol esterification rate and decreased LCAT activity has been described in a Japanese woman (18). It has also been described that chymase has the ability to cleave the C terminus of ApoA-I at Phe225, reducing its ability to promote cellular cholesterol efflux (19).

Several studies have reported the impact of changes in HDLs on CVD. Specifically, HDLs from acute coronary syndrome patients have been shown to suffer a shift to an inflammatory profile and a functional impairment linked to a remodeled protein cargo in the different HDL subfractions (20). Decreased antioxidant properties have been reported in HDLs of type 2 DM patients, a defect ascribed to tentative changes in HDL composition (21).

In this study, we hypothesized that the impaired HDL function described in DM patients might be due to structural changes in ApoA-I.

## MATERIALS AND METHODS

### DM patients and nonDM controls

The study population was comprised of a group of 55 DM patients with HbA1c >6% and a group of 58 nonDM individuals who attended to a routine health check. Diabetes mellitus was defined according to the American Diabetes Association (ADA) 1997 criteria. Standard biochemical analyses were performed in the analytical chemistry hospital laboratory. The ethics committee of the Santa Creu i Sant Pau Hospital approved the project and the studies were conducted according to the principles of the Declaration of Helsinki. All participants gave written informed consent to take part in the study.

### Blood collection and sample preparation

Venous blood samples were collected to prepare serum that was aliquoted and stored at −80°C. For proteomic studies, serum samples were prepared as previously described (22, 23). Total HDL, HDL2, and HDL3 subfractions were prepared, as previously described, in KBr density gradients of 1.063–1.210, 1.063–1.125, and 1.125–1.210, respectively (22, 23). VLDLs were isolated following the same protocol, but in a 1.006–1.019 density gradient. LDL subclasses were isolated following the same methodology as for total LDLs (density gradient of 1.019–1.063), but with density gradients of 1.019, 1.030, 1.041, and 1.052 for subfractions 1, 2, 3, and 4, respectively.

Lipoprotein purity was routinely analyzed by electrophoresis (2 μl sample) in agarose gels using a commercial assay (SAS-MX Lipo 10 kit; Helena Biosciences), as described by the providers. In addition, LDL purity was checked by analyzing the LDL profile in samples of randomly selected subjects (one subject per ultracentrifugation batch) by chromatography analysis by microgel filtration using a Superose 6 PC 3.2/30 column and an Agilent 1200 HPLC system, as previously described (24). Briefly, 10 μl of undiluted LDL sample fraction were loaded in the system and run with a constant flow of 100 μl/min. Retention time for the LDL fraction (130 min) was compared with that for HDL (134 min) and VLDL (128 min).

The method of Karlsson et al. (25) was used for VLDL and LDL protein mapping, with minor modifications. Briefly, 1 ml of either VLDLs or LDLs (1 g/l ApoB) was delipidated by mixing with 14 ml of ice-cold tributyl phosphate:acetone:methanol (1:12:1) and incubating for 90 min at −20°C, followed by centrifugation at 2,800 *g* for 15 min. Protein pellets were washed sequentially with 1 ml of tributyl phosphate, acetone, and methanol, and then air dried. Precipitates were boiled in solution containing 0.325 M DTT, 4% chaps, and 0.045 M Tris for 3 min, cooled at room temperature, diluted (1:15) in urea/thiourea/chaps solution, and incubated at 35°C for 15 min. The serum resulting after lipoprotein isolation was also collected for proteomic studies as the lipoprotein-depleted serum (LPDS) fraction.

Protein concentration was measured with a 2D-Quant kit (GE Healthcare). All processed samples were stored at −80°C until used.

### Proteomic analysis

Proteomic analysis was performed in representative subgroups of the study population in complete serum [serum; 12 DM patients (6 type 1 and 6 type 2) and 6 nonDM subjects], LPDS (N = 3 per group), and lipoprotein fractions (HDL and LDL, N ⩾ 5 per group in both cases; and VLDL, N = 3 per group). The proteomic analysis of LDL subfractions was performed in 30 DM patients and 30 nonDM individuals pooled in three groups of 10 subjects each in order to obtain enough protein.

*Two-dimensional gel electrophoresis.* For analytical and preparative gels, respectively, a protein load of 120 μg and 300 μg of the urea/chaps (for human and rat serum, and human LPDS extracts) and urea/thiourea/chaps (for human HDL, LDL, and VLDL extracts and rat liver tissue extracts) were applied to 18 cm dry strips (pH 4–7 linear range; GE Healthcare). The second dimension was resolved in 10% SDS-PAGE gels. In a subset of samples, isoelectrofocusing (IEF) was performed in a pH zoom between 4.5 and 6.9 and 15% SDS-PAGE gels to specifically focus on the ApoA-I region. Gels were developed by fluorescent staining (Flamingo; Bio-Rad). In two-dimensional gel electrophoresis (2-DE) analyses, the proteomic profile of both groups was compared by using the PD-Quest 8.0 software (Bio-Rad) that specifically analyzes the differences in protein patterns by using a single master that includes all the gels of each independent experiment (samples from control and DM patients). In this analysis, each spot in the gel is assigned a relative value that corresponds to the single spot volume compared with the volume of all spots in this gel. Afterwards, this value is subjected to background extraction and the final intensity value is then normalized by the local regression model (LOESS) method of the software.

*MS analysis.* Proteins were identified after in-gel tryptic digestion and extraction of peptides from the gel pieces, as previously

described (22, 23), by MALDI-TOF using an AutoFlex III Smartbeam MALDI-TOF/TOF (Bruker Daltonics). Samples were applied to Prespotted AnchorChip plates (Bruker Daltonics) surrounding the calibrants provided on the plates. Spectra were acquired with flexControl on reflector mode (mass range, *m/z* 850–4,000; reflector 1, 21.06 kV; reflector 2, 9.77 kV; ion source 1 voltage, 19 kV; ion source 2 voltage, 16.5 kV; detection gain, 2.37×) with an average of 3,500 added shots at a frequency of 200 Hz. Each sample was processed with flexAnalysis (v3.0; Bruker Daltonics) considering a signal-to-noise ratio over 3, applying statistical calibration, and eliminating background peaks. For identification, peaks between 850 and 1,000 were not considered because, in general, only matrix peaks are visible in this mass range. After processing, spectra were sent to the interface, BioTools (v3.2; Bruker Daltonics), and MASCOT search on Swiss-Prot 57.15 database was done [taxonomy: *Homo sapiens*, mass tolerance 50–100, up to 2 miss cleavage; global modification: carbamidomethyl (C); variable modification: oxidation (M)]. Identification was accepted with a score higher than 56. Analysis of the truncated form was investigated using the Sequence Editor tool of BioTools. For theoretical digestion of ApoA-I, the sequence reported as P02647 in Swiss-Prot was used and the parameters for peptide generation were the same as for the MASCOT search. The peptides generated in Sequence Editor were then sent back to BioTools for comparison with the experimental data and MASCOT result.

### Western blot analysis

Protein extracts were resolved by, one-dimensional gel electrophoresis (1-DE) (LDL and VLDL samples) and 2-DE (LDL, VLDL, rat serum, and liver samples) under reducing conditions and electrotransferred to polyvinylidene difluoride membranes in semi-dry conditions (semi-dry transfer system; Bio-Rad). Protein detection was performed using rabbit polyclonal antibody against total ApoA-I (178422, 1:1,000 dilution; Calbiochem) combined with the Dye Double Western blot kit (Invitrogen). Band fluorescence was determined with Typhoon FLA 9500 (GE Healthcare) and band quantification was performed using ImageQuant TL v7.01 software (GE Healthcare). Protein load was normalized using total protein fluorescent signal.

### Lipidomic analysis

Free cholesterol (FC) and TG content was analyzed by TLC, as previously described (26), in DM (N = 10) and nonDM (N = 8) subjects. Briefly, the organic solvent was removed under a $N_2$ stream and the lipid extract redissolved in dichloromethometane prior to TLC analysis that was performed on silica G-24 plates. The different concentrations of standards were applied to each plate. The chromatographic developing solution was heptane/diethyl ether/acetic acid (74:21:4, v/v/v). Bands corresponding to FC and TG were quantified using a computing densitometer (GS-800; Bio-Rad).

CE content and phospholipid species [lysophosphatidylcholine (LPC), lysophosphatidylethanolamine (LPE), lysophosphatidylserine (LPS), phosphatidylcholine (PC), phosphatidylethanolamine (PE), phosphatidylserine (PS), and SM] were assessed by LC-MS analysis in DM (N = 10) and nonDM (N = 8) subjects. To this end, lipids from LDL fractions were extracted by a modified Bligh and Dyer technique (27). After chloroform/methanol extraction, lipid extracts were analyzed by LC-MS on an Agilent 1200 HPLC system coupled to a 3200 Q-TRAP mass spectrometer. For fatty acid analysis, hydrolysis and derivatization to trimethylaminoethyl (TMAE) esters were performed prior to the separation using a Varian Pursuit diphenyl column (28). Samples were ionized using an ESI source in the positive ionization mode, and quantification was performed in the multiple reaction monitoring mode. CE and phospholipid analyses were performed on an Eclipse XDB-C18 C18 column and by MS/MS or high-resolution MS. The LIPIDVEIW database was used for identification, and normalization was performed as previously described (29).

### Quantification of ApoA-I serum levels

ApoA-I serum concentration in DM (N = 55) and nonDM (N = 59) patients was determined by competitive sandwich enzyme-linked immunosorbent assay (AssayPro) using immobilized polyclonal antibodies, as described by the providers. The detection limit of the assay was 1.2 μg/ml and the intra-assay and inter-assay coefficients of variation were 4.6 and 7.3%, respectively.

### Cathepsin D ApoA-I digestion

ApoA-I cathepsin D digestion was performed by incubating 10 μg of purified ApoA-I (ab50239; Abcam) with one unit of cathepsin D (ab77871; Abcam) in a 0.1 M sodium formate buffer for 18 h at 37°C and a pH of 3.6. Hemoglobin digestion was used as a positive control of enzyme activity. After digestion, samples were resolved in 15% SDS-PAGE gels that were developed by fluorescent staining (Flamingo; Bio-Rad).

### ApoA-I binding assay

Human recombinant ApoA-I (ab168890; Abcam) was labeled with a fluorescent dye (DyLight 488 microscale labeling kit; Thermo Scientific). After labeling, 100 μg of ApoA-I were digested with cathepsin D for 18 h at 37°C and a pH of 3.6. The same amount of labeled ApoA-I (100 μg) was incubated in the same conditions but without cathepsin D. Then, full-length and truncated labeled ApoA-I were incubated with LDL and HDL fractions for 1 h at room temperature (50 μg ApoA-I/100 μg LDL or HDL). Afterwards, unbound ApoA-I was removed by filtration with a cut-off of 100 kDa (Amicon Ultra-0.5 Centrifugal filter devices; Merck-Millipore). The fluorescent signal of the lipoprotein-ApoA-I-labeled fraction was detected with Typhoon FLA 9500 (GE Healthcare) and the amount of ApoA-I was quantified using ImageQuant TL v7.01 (GE Healthcare).

### TRAP-antioxidant capacity

Human recombinant ApoA-I (ab168890; Abcam) was incubated for 18 h at 37°C and a pH of 3.6 with or without cathepsin D. LDLs (100 μg) were oxidized with 20 μM $Cu_2SO_4$ for 4 h at 37°C, alone or in the presence of full-length ApoA-I or cathepsin D-cleaved ApoA-I. Afterwards, LDL oxidation was stopped by incubation with EDTA (1 mM) and butylated hydroxytoluene (BHT; 1 mM) for 1 h at 37°C. The antioxidant capacity of each sample (LDL alone or in the presence of full-length ApoA-I or cathepsin D-cleaved ApoA-I) was assessed by the total peroxyl radical-trapping antioxidant potential (TRAP) method. Briefly, DCFH-DA (D-399; Invitrogen) was prepared by basic hydrolysis and added to the sample at 10 μM. After an incubation period (2 h at 37°C), TRAP was determined with Typhoon FLA 9500 (GE Healthcare) and quantified using ImageQuant TL v7.01 (GE Healthcare). The antioxidant capacity of cathepsin D was also assessed in order to avoid potential confounding effects.

### Rat model and hepatic tissue extraction for cathepsin D activity measurement

Zucker diabetic fatty rats (N = 7) and their corresponding lean normoglycemic controls (N = 8) were fed with LabDiet® 5008 chow and water given ad-libitum with 12 h day/night cycles. Animals were anesthetized with a combination of ketamine and medetomidine (75 mg/kg and 0.5 mg/kg, ip) and then euthanized with an intracardiac overdose of sodium pentobarbital. Liver samples were extracted immediately after the animals were euthanized, and immediately frozen in liquid nitrogen and stored at −80°C.

All animals were purchased from Charles River Laboratories. All procedures fulfilled the criteria established by the *Guide for the Care and Use of Laboratory Animals* published by the US National Institutes of Health (NIH Publication No.85-23, revised 1996) and were approved by the Internal Animal Committee Review Board.

Frozen liver samples from diabetic and control animals were pulverized and homogenously distributed in aliquots for protein extraction. Pulverized tissue was homogenized in a lysis buffer containing 0.4% chaps for the cathepsin D activity assay, and in a urea/thiourea/chaps buffer for the 2-DE analysis. Protein concentration was measured using the 2D-Quant kit (GE Healthcare). Cathepsin D activity in hepatic protein extracts was measured using a commercially available cathepsin D assay kit (Sigma) following the provider's instructions.

### Statistical analysis

Data are expressed as median [interquartile range] unless stated otherwise. N indicates the number of subjects/animals tested. Statistical analysis was performed with Stat View 5.0.1 software. Statistical differences between groups were analyzed by the nonparametric Mann-Whitney or Kruskal-Wallis tests for multiple comparisons. Chi-square test ($\chi^2$) or Fisher's exact test, when any of the expected values were <5, were used for categorical variables. $P \leqslant 0.05$ was considered significant.

To determine correlation between ApoA-I, anthropometric parameters (age and gender), risk factors (hypertension, dyslipemia, tabaco), and background medication, we performed a bivariate analysis (correlation or *t*-test) followed by a multiple linear regression model (stepwise selection of variables), including those variables statistically significant in the bivariate analysis to assess the most parsimonious model.

## RESULTS

### Characteristics of the studied population

Characteristics of DM and control nonDM patients participating in this study are shown in **Table 1**. Patients were treated as per guideline recommendations.

### ApoA-I proteomic profile in DM patients

Proteomic analysis by 2-DE (pH ranges 4–7 and 4.7–5.9; supplementary Fig. 1) of serum samples revealed ApoA-I as a cluster of five spots with the same apparent molecular mass of 28 kDa and a isoelectric point (pI) range between 5 and 5.75, as previously reported (23). By MALDI-TOF analysis, the five spots were identified as ApoA-I in both DM and nonDM subjects. The ApoA-I proteomic profile in both groups was compared (**Fig. 1A, B**). Spot 5 showed a 46% increase in its intensity in DM patients when compared with nonDM subjects ($P < 0.01$; Fig. 1C). This significant difference was not picked-up by ELISA determination of ApoA-I serum levels that gave significantly lower values in DM patients when compared with nonDM individuals (DM: 69.8 [59.8–83.5] mg/dl vs. nonDM: 139.7 [119.0–155.3] mg/dl, $P < 0.0001$; Table 1).

Multiple linear regression analysis, including those variables statistically significant for ApoA-I serum levels in the bivariate analysis (risk factors and background medication), showed that only the presence of diabetes and tobacco smoking remained as independent factors for ApoA-I levels, with an R squared of 0.558. Unstandardized coefficients gave a β-value of −0.696 ($P < 0.0001$) for the presence of diabetes and −0.134 ($P < 0.05$) for tobacco smoking.

### ApoA-I truncated form

MALDI-TOF analysis of the DM patients' serum proteome revealed a spot with a pI of 5.75 and an apparent molecular mass of approximately 26 kDa (spot 6 in **Fig. 2A**) that was identified as ApoA-I with a score of 108 (10/23 peaks matched, a sequence coverage of 34.8% and an intensity coverage of 60.5%). This spot showed a 64% increase in its intensity in DM patients ($P < 0.01$; Fig. 2B), representing 4.8% of total ApoA-I in comparison with the 1.3% in nonDM subjects.

Tryptic digestion of spots 1–5 of ApoA-I generated a peptide corresponding to aa residues 37-47 that was detected as a peak of *m/z* 1,235.63 (**Fig. 3**). Spots 1–5 have been previously described in the literature (30) as the pro-ApoA-I (spots 4 and 5 in Fig. 1A, B) and the mature ApoA-I (spots 1–3 in Fig. 1A, B) forms of 28 kDa. The peak of *m/z* 1,235.63 was not detected in the mass spectra obtained from the digestion of spot 6 (Fig. 2C). As the molecular mass of spot 6 (Fig. 2A) suggested a truncated form of ApoA-I, we performed an in silico analysis using the Sequence Editor tool of BioTools (Bruker Daltonics; BioTools 3.02) simulating the tryptic sequential digestion of the N-terminal aas from ApoA-I. In this analysis, we obtained a theoretical set of peptides and their corresponding peak list (supplementary Table 1) that were compared with the experimentally obtained spectra. The theoretical pick list obtained from a truncation from aa 1 to aa 38 contained a peak of *m/z* 1,422.735, corresponding to aas from 39 to 51 (Fig. 3). This peak was found within the nonmatched peak list of spot 6. Moreover, the absence of the 38 first aas corresponded with a molecular mass of 26.4 kDa, in agreement with the molecular mass observed in 2-DE gels of spot 6 [ApoA-IΔ(1-38)].

Multiple linear regression analysis, including those variables statistically significant for ApoA-IΔ(1-38) intensity in the bivariate analysis (hypertension, dyslipemia, and insulin and Ezetrol treatment) showed that only the presence of diabetes remained as an independent factor for ApoA-IΔ(1-38) levels, with an R squared of 0.362 and an unstandardized coefficient with a β-value of 0.632 ($P < 0.01$).

### Differential ApoA-IΔ(1-38)-associated lipoprotein profile in DM patients

When total serum, LPDS, HDL, and LDL samples were analyzed in a 2-DE zoom of pH between 4.7 and 5.9, this ApoA-IΔ(1-38) form was detected in both serum and LDL, but not in LPDS or in HDL (**Fig. 4A**). The presence of the ApoA-IΔ(1-38) form in LDL extracts was confirmed by Western blot analysis of both 1-DE and 2-DE (Fig. 4B). The absence of ApoA-IΔ(1-38) in VLDL particles was confirmed by MALDI-TOF and Western blot analysis (supplementary Fig. 2).

The analysis of the LDL sub-proteome (2-DE analysis in the range of 150–20 kDa; supplementary Fig. 3) revealed a

TABLE 1. Background description of DM patients and nonDM individuals

| | DM (N = 55) | NonDM (N = 59) | *P* |
|---|---|---|---|
| Age | 55 ± 1.4 | 62 ± 1.1 | <0.0001 |
| Sex (females/males) | 23/32 | 14/44 | <0.05 |
| Risk factors (%) | | | |
| Diabetes (type 1/type 2) | 100 (35/65) | 0 | <0.0001 |
| Dyslipemia | 87 | 52 | <0.0001 |
| Hypertension | 93 | 21 | <0.0001 |
| Tobacco smoking | 49 | 17 | <0.0001 |
| History of CVD (%) | 4 | 0 | NS |
| BMI | 26 ± 0.4 | 27 ± 0.5 | <0.05 |
| Total-C (mg/dl) | 182 ± 4.5 | 217 ± 5.3 | <0.0001 |
| HDL-C (mg/dl) | 53 ± 2.2 | 49 ± 1.9 | NS |
| LDL-C (mg/dl) | 101 ± 3.4 | 143 ± 4.6 | <0.0001 |
| TGs (mg/dl) | 129 ± 17.1 | 130 ± 12.0 | NS |
| ApoA-I (mg/dl) | 69 ± 2.9 | 147 ± 5.9 | <0.0001 |
| Glucose (mg/dl) | 157 ± 7 | 87 ± 2.8 | <0.0001 |
| HbA1c (%) | 7.6 ± 0.1 | — | — |
| Background medication (%) | | | |
| OADs | 58 | 0 | <0.0001 |
| INS | 80 | 0 | <0.0001 |
| Statins | 82 | 26 | <0.0001 |
| Antiaggregants | 36 | 0 | <0.0001 |
| ACEIs | 56 | 7 | <0.0001 |
| A2RAs | 62 | 3 | <0.0001 |
| $Ca^{2+}$ antagonists | 42 | 0 | <0.0001 |
| β-blockers | 7 | 2 | NS |
| Ezetrol | 29 | 0 | <0.0001 |

Data are expressed as mean ± SEM. ACEIs, angiotensin-converting enzyme inhibitors; A2RAs, angiotensin 2 receptor antagonists; INS, insulin; OADs, oral antidiabetic drugs; Total-C, total-cholesterol; HDL-C, HDL-cholesterol; LDL-C, LDL-cholesterol.

significant increase in the intensity of ApoA-IΔ(1-38) spot in DM patients when compared with nonDM individuals (DM: 1.74 [1.54–2.04] AU vs. nonDM: 1.01 [0.87–1.14] AU; $P < 0.05$; Fig. 4C). ApoB-100 (molecular mass of 515 kDa) does not appear because it is out of the range of the 2-DE analysis used here, that was selected to obtain the ApoA-I profile.

### Lipidomic characterization

A lipidomic approach was further used to characterize LDL preparations from DM and nonDM subjects. LDLs from DM patients showed no significant changes in the content of TG and FC levels measured by TLC (supplementary Fig. 4A), but showed higher CE levels measured by LC-MS than nonDM individuals ($P < 0.05$; supplementary Fig. 4B).

### Lipoprotein subclasses and ApoA-IΔ(1-38)

In order to analyze whether ApoA-IΔ(1-38) was differentially distributed in the different LDL subclasses and to probe its absence in all HDL subclasses, proteomic analysis of four LDL (LDL1–LDL4) and two HDL (HDL2 and HDL3) subtypes was performed. ApoA-IΔ(1-38) was not detected in the HDL2 or in the HDL3 subfraction (supplementary Fig. 5). When the four LDL subclasses were analyzed (pI range of 4–7 and 10% PAGE), ApoA-IΔ(1-38) was differentially distributed between DM and nonDM subjects (**Fig. 5A**). In nonDM individuals, ApoA-IΔ(1-38) was equally distributed along the different LDL subclasses, while DM patients depicted a significant increase in the intensity of ApoA-IΔ(1-38) in the denser LDL subtypes (LDL3 and LDL4; $P < 0.05$; Fig. 5B) when compared with the nonDM group. The sum of the intensities of ApoA-IΔ(1-38) in all the LDL fractions reproduced the results obtained with total LDLs, with a significant increase in DM patients ($P < 0.05$; Fig. 5C). There was a differential distribution profile of lipid species in LDL subclasses between DM and nonDM subjects (**Table 2**). DM patients showed a higher content of PSs and LPSs in the LDL2 subfraction when compared with nonDM subjects ($P < 0.05$). The LDL3 subfraction depicted a significant increase in PCs, LPCs, and SMs, together with a decrease in PEs and LPEs in DM patients when compared with the nonDM group ($P < 0.05$).

### Cathepsin D cleaves ApoA-I and shows increased liver activity in diabetic rats

Data mining analysis opened tentative pathways to explain the posttranscriptional truncation of ApoA-I. An experimental model of diabetes was used to proof the concept. First, the proteomic profile of rat serum revealed the presence of two ApoA-I forms of 28 and 26 kDa, similar to the forms (molecular mass) observed in human serum (supplementary Fig. 6A). Rat ApoA-I behaves differently in the proteomic profile due to the already described differences in the pI of the pro-ApoA-I (full-length) and the mature ApoA-I forms. As stated in the protein database UniProt, the mature form of human ApoA-I (aas 25-267; SwissProt accession number, P02647) has a more acid pI (5.27) than pro-ApoA-I (full-length; aas 19-267; pI 5.45). In contrast, in rat, the mature form of ApoA-I (aas 25-259; accession number, P04639) has a more basic pI (5.51) than pro-ApoA-I (full-length; aas 19-259; pI 5.41), giving an inverted proteomic profile in the 2-DE analysis as a result. Therefore, our results showed that the truncated low molecular mass ApoA-I form of 26 kDa is detected in both cases underneath the full-length

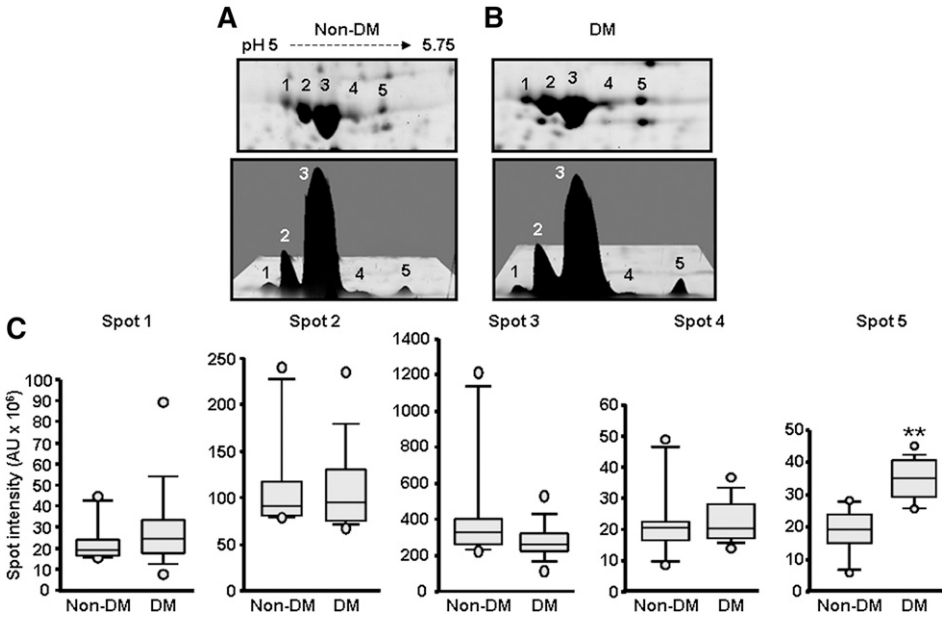


**Fig. 1.** Representative serum 2-DE images (pI range 4–7, 10% PAGE) of ApoA-I spots in nonDM subjects (N = 6) (A) and DM-patients [N = 12 (6 type 1 and 6 type 2)] (B). C: Box-plot diagrams showing the intensity of each spot in both groups. Spot 5 was significantly increased in DM patients. $^{**}P < 0.01$.

ApoA-I form (pro-ApoA-I). As in humans, diabetic rats showed significantly higher levels of the ApoA-I form of 26 kDa in serum than nondiabetic rats ($P < 0.05$; supplementary Fig. 6B). This observation led us to investigate the potential enzymes involved in the cleavage of both human and rat ApoA-I molecules. In silico analysis using MEROPS database (31) revealed cathepsin D as the only enzyme able to cleave ApoA-I sequence from both species (supplementary Fig. 6C).

In vitro treatment of ApoA-I with cathepsin D abolished the 28 kDa ApoA-I form and led to the detection of a lower molecular mass band in agreement with the 2-DE profile of both ApoA-I forms (supplementary Fig. 7A). The activity of cathepsin D was controlled by using hemoglobin digestion as a positive control.

As ApoA-I is synthesized in the liver, hepatic cathepsin D activity in diabetic rats was analyzed in order to test whether ApoA-I could be cleaved after synthesis. Diabetic rats showed a significant increase in hepatic cathepsin D activity when compared with control animals (diabetic rats: 6.1 [4.2–6.7] vs. control animals: 3.71 [2.7–4.8]; $P < 0.05$; supplementary Fig. 7B).

Additionally, the ApoA-I proteomic profile (2-DE followed by ApoA-I Western blot analysis) of rat liver samples revealed the presence of the same ApoA-I forms of 28 and 26 kDa (supplementary Fig. 7C) with the same distribution as the one detected in rat serum. Diabetic rats showed a 2-fold increase in the hepatic content of the ApoA-I form of 26 kDa compared with control animals ($P < 0.05$; supplementary Fig. 7D).

### Cathepsin D-cleaved ApoA-I exhibits increased LDL binding ability and diminished antioxidant properties

In order to proof the differential affinity toward different lipoproteins of truncated ApoA-I, we performed in vitro experiments with full-length recombinant ApoA-I and cathepsin D-cleaved ApoA-I. Truncated ApoA-I showed a 39% lower binding ability toward HDLs than the full-length ApoA-I. On the contrary, cathepsin D-cleaved ApoA-I exhibited a 47% higher binding capacity toward LDLs when compared with full-length ApoA-I ($P < 0.0001$ for all comparisons; **Fig. 6A**).

We further analyzed the potential functional implication of this increased binding affinity of truncated ApoA-I toward LDLs by measuring the antioxidant capacity against LDL oxidation of both full-length and cathepsin D-cleaved ApoA-I. Cathepsin D-cleaved ApoA-I truncation resulted in a 1.4-fold decrease in its antioxidant capacity, when compared with full-length ApoA-I ($P < 0.0001$; Fig. 6B).

## DISCUSSION

The functional activity of HDLs has been repeatedly reported as defective and as a contributor to the high cardiovascular risk of DM patients (21). In this study, we have approached the investigation by proteomics and lipidomics of the ApoA-I profile and found important changes in its isoform distribution pattern in DM patients. Interestingly, here we describe for the first time the presence of ApoA-IΔ(1-38) in serum, a form that is significantly increased in DM patients. ApoA-I is modified at a post-translational level (32) and several environmentally/metabolically related modifications have been reported, such as fatty acid acylation (33) and oxidation (34). In DM patients, attention has been focused on nonenzymatic protein glycation and advanced glycation end product (AGE) formation. Both are related to hyperglycemia in type 1 and type 2 diabetes, where AGE adducts are associated with ApoA-I, impairing its ability to activate LCAT,

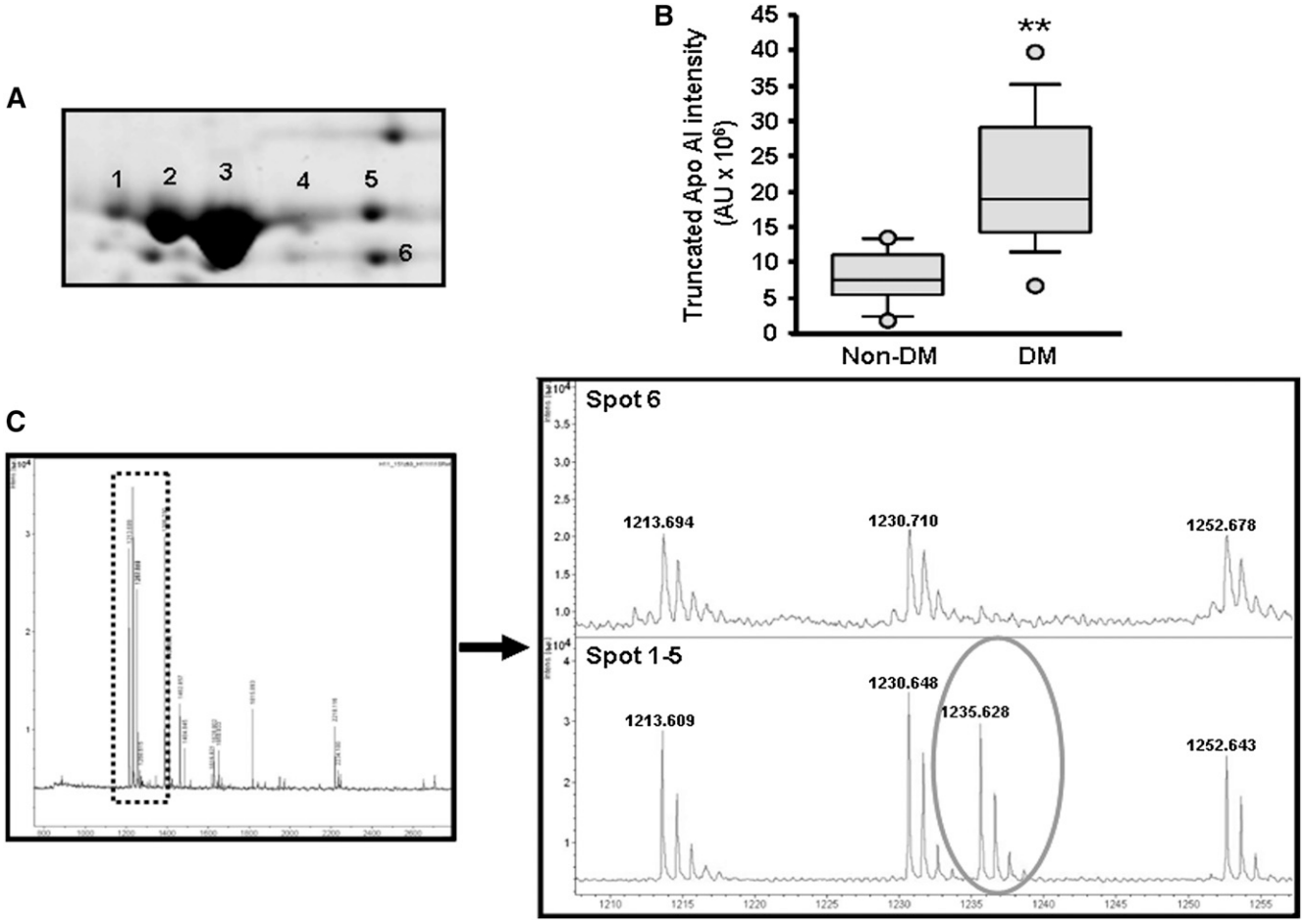


**Fig. 2.** A: Representative serum 2-DE image (pI range 4–7, 10% PAGE) showing ApoA-I spot 6 at 26 kDa. B: Box-plot diagram showing the increase in spot 6 intensity in DM patients. $^{**}P < 0.01$. C: MALDI-TOF spectra of human serum ApoA-I. D: Enlarged image showing the absence of the $m/z$ 1,235.63 peak in spot 6 compared with spots 1–5.

the enzyme responsible for converting nascent HDLs into mature HDLs (35). AGEs seem to accelerate the development of CAD (36). ApoA-I modification studies have also shown that the most basic forms are the less mature isoforms of the protein (30). Interestingly, we have detected an increase in the basic less mature form of ApoA-I in diabetics.

Proteolysis is thought to play an important role in most types of amyloidoses, in atherosclerosis, and in neurodegenerative diseases. In fact, macrophage metalloproteinases degrade HDL-associated ApoA-I at both the N and C termini in coronary patients (37). Intriguingly, ApoA-IΔ(1-38), lacking residues 1-38, is significantly increased in serum samples of DM patients, and it is found associated to LDL lipoproteins and not to VLDL or HDL micelles. In vitro studies have demonstrated that the experimental deletion of residues 1-43 from ApoA-I results in a less stable tertiary structure than full-length ApoA-I (38). Moreover, the deletion mutants lacking residues 1-41 and 1-59 showed altered lipid binding ability compared with wild-type ApoA-I (39). The N-terminal 44 aa sequence of ApoA-I is predicted to be responsible for the stabilization of soluble ApoA-I; and recently, it has been demonstrated that residues 35-49 play a role in the adaptation of ApoA-I to the particle size of HDLs (10). Therefore, the lack of the 38 first aas detected in ApoA-IΔ(1-38) may affect the transition from lipid-free ApoA-I to spherical HDL particles (40) (**Fig. 7**), potentially impairing the reverse cholesterol transport ability and facilitating its binding to LDL particles. Indeed, our in vitro experiments have demonstrated a diminished binding ability of the truncated ApoA-I form to HDLs, together with an important increase in its binding to LDLs, when compared with full-length ApoA-I. These results indicate that, after truncation, there is a selective binding of ApoA-IΔ(1-38) to LDLs and not an incorporation into LDLs during the particle formation process, as ApoA-IΔ(1-38) is not associated to VLDLs.

The N-terminal aas are necessary for formation of large HDL complexes, and their absence leads to less stable HDL particles (41). Although, traditionally, ApoA-I has been related to HDLs as the main protein component in these micelles, previous studies have reported the presence of this apolipoprotein in LDL particles (25). Interestingly, in the present study, DM patients showed a strong decrease in total ApoA-I serum levels, measured by ELISA, when compared with healthy individuals independently of background medication. Moreover, DM patients showed similar HDL-cholesterol levels to the control

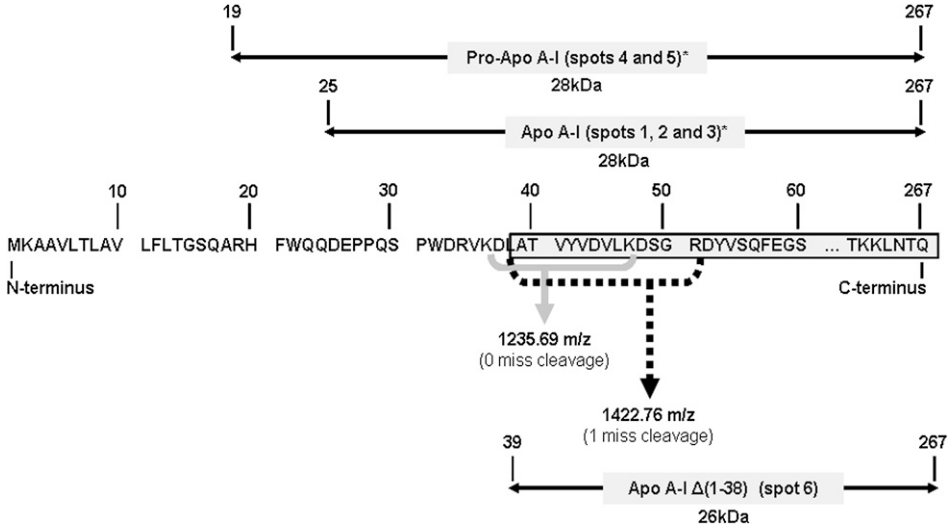


**Fig. 3.** Scheme showing the truncation of aas 1-38 in ApoA-I sequence and the fragments corresponding to the peaks detected in MALDI-TOF analysis. *Previously described ApoA-I forms (30) include: Pro-ApoA-I (aas 19-267) that corresponds to spots 4 and 5 in Fig. 1A, B, and mature ApoA-I (aas 25-267) that corresponds to spots 1, 2, and 3 in Fig. 1A, B. Spot 6 in Fig. 2A (identified here), corresponds to aas from 39 to 267, ApoA-IΔ(1-38).

group, highlighting the discordance between levels, structure and function, and the relevance of HDL quality rather than its quantity (4). These results emphasize the potential implication of this decrease in ApoA-I levels in the increased cardiovascular risk of DM patients and the inconsistency of measuring cholesterol transported by HDLs as an index of HDL particle content, and even more of its afforded atheroprotection. Indeed, some studies are already relating not HDL but Apo A-I levels to a worse prognosis in DM patients (42). Furthermore, this and previous (23) studies of our group underscore that the measurement of specific forms (immature and truncated forms in diabetes) would better help in the prognostic value of ApoA-I.

In this study, we have also demonstrated for the first time that cathepsin D can cleave ApoA-I and potentially increase ApoA-IΔ(1-38) that is associated to LDL particles in DM patients later on, due to its increased binding ability. Previous studies have demonstrated an increase in cathepsin D activity to cleave hemoglobin in serum samples of DM patients (43). Herein, we have found increased cathepsin D activity in the liver of diabetic rats together with an increased content of truncated ApoA-I, both in liver and serum. These findings, together with the previously described increased susceptibility of the N-terminal region of lipid-free ApoA-I to protease cleavage (44), leads us to speculate that once synthesized, ApoA-I is cleaved by cathepsin D either at the liver or in the circulation, producing an ApoA-I particle lacking the first 38 aas, with increased affinity for LDLs. Thus, this truncation may lead to the binding of the ApoA-IΔ(1-38) form to LDL particles, yielding an LDL population more prone to oxidation

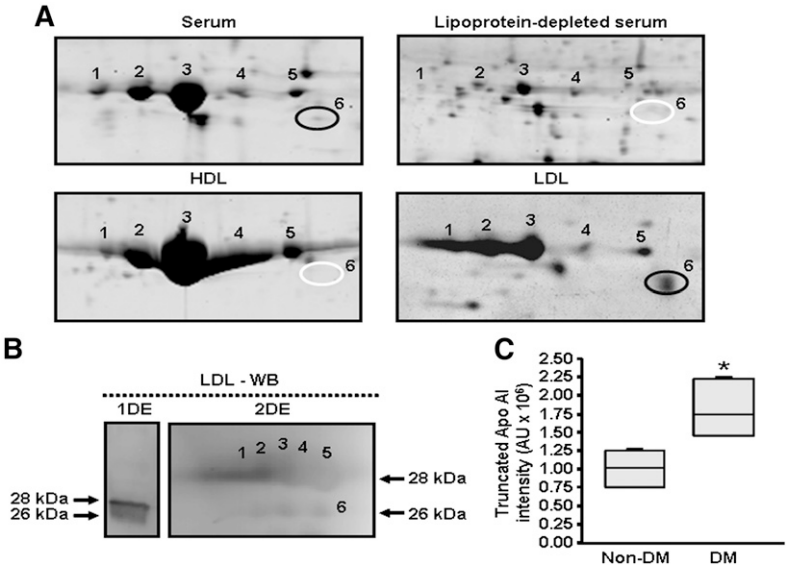


**Fig. 4.** A: Representative 2-DE image (pI range 4.7–5.9, 15% PAGE) of ApoA-I profile in serum, LPDS (N = 3 per group), HDL (DM, N = 6; nonDM, N = 9), and LDL (N = 5 per group) samples showing ApoA-IΔ(1-38) presence in serum and LDLs. B: Representative 1-DE and 2-DE Western blot (WB) images showing ApoA-I at 28 and 26 kDa in LDL samples. C: Box-plot diagram of the ApoA-IΔ(1-38) increase in LDLs of DM patients. *$P < 0.05$.

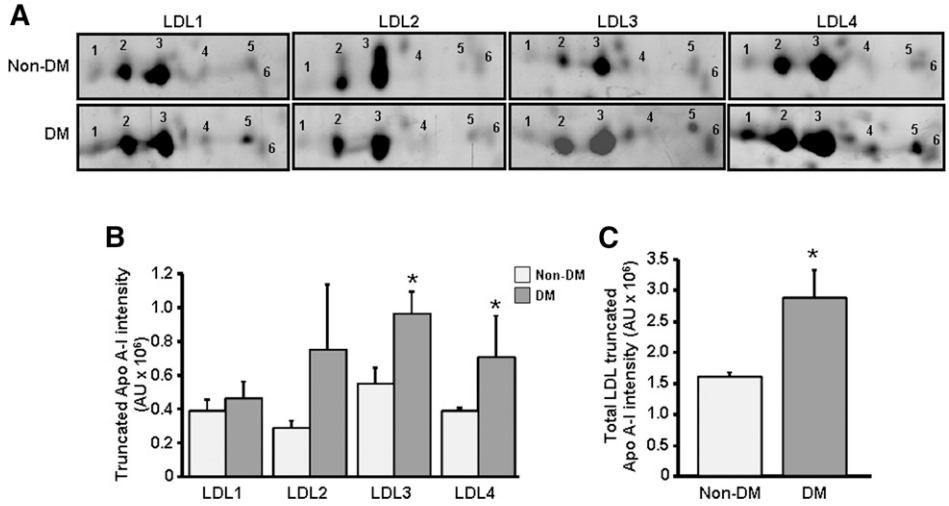


**Fig. 5.** A: Representative 2-DE image (pI range 4–7, 10% PAGE) of ApoA-I in LDL subclasses in DM patients and nonDM subjects (30 DM patients and 30 nonDM individuals pooled in three groups of 10 subjects each). Bar diagrams showing the significant increase in ApoA-IΔ(1-38) intensity in LDL3 and LDL4 of DM patients (B) and in the sum of ApoA-IΔ(1-38) intensity in all the LDL subfractions (C). $*P < 0.05$.

and contributing to the already described modified LDL particles in DM patients. Indeed, it has been suggested previously that cathepsin D could induce hydrolytic modifications of LDLs, favoring the formation of foam cells in the intima of human arteries (45). Moreover, cathepsin D has been shown to be released by atherosclerotic plaques, and increased plasma levels have been found in acute coronary syndrome patients (46). Although we have found a potential role of cathepsin D in the formation of ApoA-IΔ(1-38), we cannot exclude the implication of other enzymes.

Several studies have reported different LDL modifications in diabetics due to oxidation and glycosylation, resulting in the presence of more atherogenic LDL particles in these patients (47). Indeed, the increased cardiovascular risk of DM patients has been related to the presence of small dense LDL particles (48), which have been shown to be more atherogenic and may explain, at least in part, the higher risk of those patients even having similar LDL-cholesterol plasma concentrations than control subjects (49). Specifically, the formation of small dense LDL particles in type 2 diabetes has been attributed to a preferential CE transfer from HDLs to small dense LDLs (50). Indeed, our lipidomic analysis has revealed an increase in the CE content in LDLs from DM patients. Furthermore, it has been shown that small dense LDL particles exhibit a higher affinity for arterial proteoglycans, a fact that could increase its susceptibility to being retained in the intima, a determinant step in atherogenesis (51). Importantly, our proteomic profiling approach has revealed that DM patients have higher ApoA-IΔ(1-38) content in the denser LDL fractions (LDL3 and LDL4) probably contributing to the modification of such lipoproteins in relation to diabetes. The increase in the content of ApoA-IΔ(1-38) together with the decrease in total ApoA-I serum levels could induce an increase in the susceptibility to LDL atherogenic modifications, as ApoA-I has been postulated to enter the vessel wall and protect LDLs in the arterial wall (52). In this context, the increase in truncated ApoA-I in DM patients could lead to a higher LDL oxidation level, as suggested by our in vitro studies. In fact, previous studies have proposed the existence of several ApoA-I truncated forms and their potential implication in the assessment of cardiovascular risk (44). In addition, our lipidomic analysis

TABLE 2. Lipidic distribution profile in LDL subclasses of DM patients and nonDM individuals

| | Lipid Content (μg/mg of protein) | | | |
|---|---|---|---|---|
| | LDL1 | LDL2 | LDL3 | LDL4 |
| NonDM | | | | |
| CE | 1,884.1 [1,477.8–2,290.5] | 1,251.0 [8,91.0–1,704.2] | 906.9 [812.1–988.0] | 2,536.5 [2,445.7–2,627.3] |
| PC, LPC, SM | 200.7 [195.3–206.1] | 121.3 [107.3–137.8] | 176.8 [173.6–180.2] | 278.8 [256.7–300.9] |
| PE, LPE | 3.3 [3.0–3.6] | 1.2 [1.0–1.7] | 0.8 [0.7–1.0] | 1.2 [1.1–1.3] |
| PS, LPS | 31.9 [29.1–34.7] | 8.0 [6.9–11.6] | 3.5 [3.3–6.8] | 26.6 [18.1–35.1] |
| DM | | | | |
| CE | 774.9 [748.5–801.4] | 1,610.5 [1,384.4–1,641.9] | 1,319.3 [1,011.4–1,408.2] | 1,882.0 [1,383.5–2,250.4] |
| PC, LPC, SM | 296.2 [295.6–296.9] | 256.1 [202.8–350.3] | 233.7 [221.1–235.5][a] | 324.3 [226.2–345.7] |
| PE, LPE | 1.7 [1.6–1.7] | 0.8 [0.7–0.8] | 0.5 [0.5–0.5][a] | 1.1 [1.0–1.2] |
| PS, LPS | 42.4 [37.4–47.4] | 19.1 [18.8–20.5][a] | 8.1 [7.9–9.6] | 19.3 [17.7–19.5] |

Data are expressed as median [interquartile range].
[a] $P = 0.049$, Mann-Whitney, DM versus NonDM.

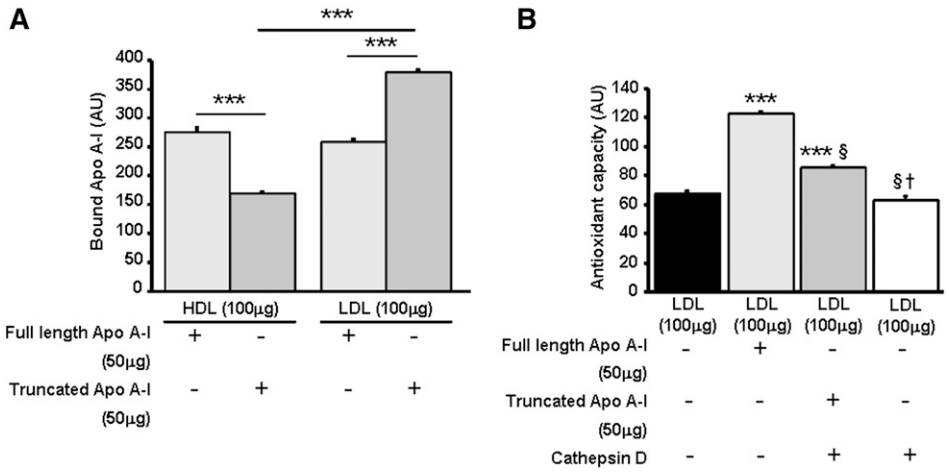


**Fig. 6.** Bar diagrams showing: the differential binding ability of full-length and cathepsin D-cleaved ApoA-I to HDLs and LDLs (***$p$<0.0001 for all comparisons; N = 3 independent experiments) (A); and the significant decrease in ApoA-I antioxidant capacity against LDL oxidation after cathepsin D truncation (***$P$ < 0.0001 vs. LDL; §$P$ < 0.0001 vs. full-length ApoA-I; †$P$ < 0.0001 vs. truncated ApoA-I; N = 3 independent experiments) (B).

has revealed changes in the content of several lipid species in different LDL subclasses, with a specific increase of the proinflammatory molecule LPC, among others, in LDL3 of DM patients. Interestingly, LPC has previously been shown to be associated with oxidized LDL particles playing a key role in atherosclerosis and the inflammatory response (53).

The main limitation of the present study refers to the existence of differences in the baseline characteristics between DM and nonDM patients. However, despite the potential influence of these parameters in ApoA-I metabolism, the multivariate statistical analysis has revealed the presence of diabetes as the main parameter influencing ApoA-IΔ(1-38) levels.

Previous studies have already proved the increased atherogenic properties of small dense LDL particles of DM patients (54). This study highlights the potential relevance of ApoA-I truncated forms in relation to this increased cardiovascular risk of DM patients. Moreover, our results point to the potential implication of cathepsin D in ApoA-IΔ(1-38) formation. Possibly, other proteases may also cleave ApoA-I sequence at the same site.

Unfortunately, the amount of material obtained in the 2-DE analysis corresponding to ApoA-IΔ(1-38) is too low to allow us to perform N-terminal sequencing analysis. Nevertheless, the molecular mass profile observed in the 2-DE analysis agrees with a truncated ApoA-I form that has also been confirmed by the differential trypsin digestion peptide profile observed in MS analysis.

In summary, despite the limitations of 2-DE approaches for the study of such a complex sample like serum, by careful use of biochemical analysis, we have obtained useful complementary information about the presence of protein variants in diabetes. Thus, we have described, for the first time, the increase of a 26 kDa N-terminal truncated form of ApoA-I that we have named ApoA-IΔ(1-38) that associates to the denser LDL particles in DM patients which may have effects in lipoprotein particle turnover, increase LDL susceptibility to oxidation, and further contribute to a higher cardiovascular risk. The presence of cleaved ApoA-I variants is closely related to the incidence of chronic diseases such as diabetes, atherosclerosis, and ageing (55). Therefore the potential role of this truncated

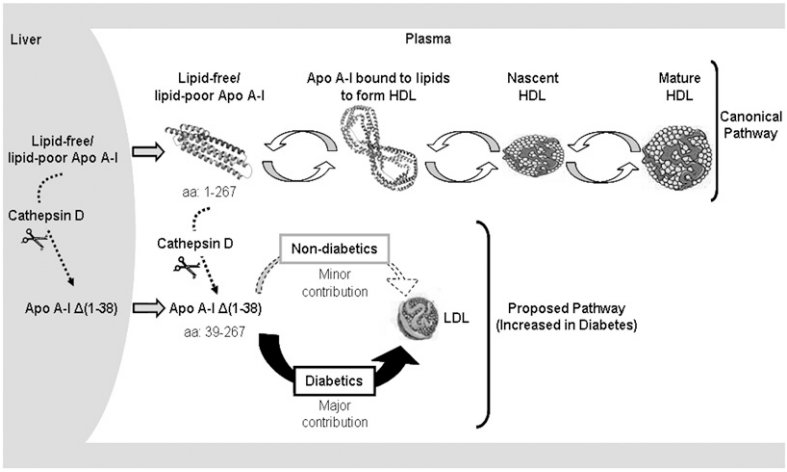


**Fig. 7.** Scheme of the canonical pathway of the conversion of an ApoA-I molecule into mature HDL micelles showing the proposed pathway of the binding of ApoA-IΔ(1-38) to LDL particles.

ApoA-I form in the pathogenesis of CVD deserves further investigation.

The authors are indebted to María Dolores Fernández, Esther Gerbolés, Estefania Segalés, Anna Navarrete, Onna Catot, Joaquim Gordo, and Rodrigo Hernández-Vera for their technical support. The authors also thank Fundación de Investigación Cardiovascular (FIC)-Fundacion Jesús Serra, Barcelona, for their continuous support.

## REFERENCES

1. Geiss, L. S., W. H. Herman, and P. J. Smith. 1995. Mortality in non-insulin-dependent diabetes. *In* Diabetes in America. 2nd edition. M. I. Harris, C. C. Cowie, M. P. Stern, et al., editors. US Government Printing Office, Washington, DC. 233–257.
2. Kannel, W. B., and D. L. McGee. 1979. Diabetes and glucose tolerance as risk factors for cardiovascular disease: the Framingham study. *Diabetes Care.* **2:** 120–126.
3. Yusuf, S., S. Hawken, S. Ounpuu, T. Dans, A. Avezum, F. Lanas, M. McQueen, A. Budaj, P. Pais, J. Varigos, et al. 2004. Effect of potentially modifiable risk factors associated with myocardial infarction in 52 countries (the INTERHEART study): case-control study. *Lancet.* **364:** 937–952.
4. Badimon, L., and G. Vilahur. 2012. LDL-cholesterol versus HDL-cholesterol in the atherosclerotic plaque: inflammatory resolution versus thrombotic chaos. *Ann. N. Y. Acad. Sci.* **1254:** 18–32.
5. Turner, R. C., H. Millns, H. A. Neil, I. M. Stratton, S. E. Manley, D. R. Matthews, and R. R. Holman. 1998. Risk factors for coronary artery disease in non-insulin dependent diabetes mellitus: United Kingdom Prospective Diabetes Study (UKPDS: 23). *BMJ.* **316:** 823–828.
6. Castelli, W. P., R. J. Garrison, P. W. Wilson, R. D. Abbott, S. Kalousdian, and W. B. Kannel. 1986. Incidence of coronary heart disease and lipoprotein cholesterol levels. The Framingham Study. *JAMA.* **256:** 2835–2838.
7. Lund-Katz, S., and M. C. Phillips. 2010. High density lipoprotein structure-function and role in reverse cholesterol transport. *Subcell. Biochem.* **51:** 183–227.
8. Davidson, W. S., and T. B. Thompson. 2007. The structure of apolipoprotein A-I in high density lipoproteins. *J. Biol. Chem.* **282:** 22249–22253.
9. Rothblat, G. H., F. H. Mahlberg, W. J. Johnson, and M. C. Phillips. 1992. Apolipoproteins, membrane cholesterol domains, and the regulation of cholesterol efflux. *J. Lipid Res.* **33:** 1091–1097.
10. Lagerstedt, J. O., G. Cavigiolio, M. S. Budamagunta, I. Pagani, J. C. Voss, and M. N. Oda. 2011. Structure of apolipoprotein A-I N terminus on nascent high density lipoproteins. *J. Biol. Chem.* **286:** 2966–2975.
11. Mulya, A., J. Y. Lee, A. K. Gebre, M. J. Thomas, P. L. Colvin, and J. S. Parks. 2007. Minimal lipidation of pre-beta HDL by ABCA1 results in reduced ability to interact with ABCA1. *Arterioscler. Thromb. Vasc. Biol.* **27:** 1828–1836.
12. Glomset, J. A. 1962. The mechanism of the plasma cholesterol esterification reaction: plasma fatty acid transferase. *Biochim. Biophys. Acta.* **65:** 128–135.
13. Badimon, J. J., L. Badimon, and V. Fuster. 1990. Regression of atherosclerotic lesions by high density lipoprotein plasma fraction in the cholesterol-fed rabbit. *J. Clin. Invest.* **85:** 1234–1241.
14. Nissen, S. E., T. Tsunoda, E. M. Tuzcu, P. Schoenhagen, C. J. Cooper, M. Yasin, G. M. Eaton, M. A. Lauer, W. S. Sheldon, C. L. Grines, et al. 2003. Effect of recombinant ApoA-I Milano on coronary atherosclerosis in patients with acute coronary syndromes: a randomized controlled trial. *JAMA.* **290:** 2292–2300.
15. Kozarsky, K. F., M. H. Donahee, A. Rigotti, S. N. Iqbal, E. R. Edelman, and M. Krieger. 1997. Overexpression of the HDL receptor SR-BI alters plasma HDL and bile cholesterol levels. *Nature.* **387:** 414–417.
16. Schultz, J. R., J. G. Verstuyft, E. L. Gong, A. V. Nichols, and E. M. Rubin. 1993. Protein composition determines the anti-atherogenic properties of HDL in transgenic mice. *Nature.* **365:** 762–764.
17. Bojanovski, D., R. E. Gregg, G. Ghiselli, E. J. Schaefer, J. A. Light, and H. B. Brewer, Jr. 1985. Human apolipoprotein A-I isoprotein metabolism: proapoA-I conversion to mature apoA-I. *J. Lipid Res.* **26:** 185–193.
18. Moriyama, K., J. Sasaki, Y. Takada, A. Matsunaga, J. Fukui, J. J. Albers, and K. Arakawa. 1996. A cysteine-containing truncated apo A-I variant associated with HDL deficiency. *Arterioscler. Thromb. Vasc. Biol.* **16:** 1416–1423.
19. Usami, Y., K. Matsuda, M. Sugano, N. Ishimine, Y. Kurihara, T. Sumida, K. Yamauchi, and M. Tozuka. 2011. Detection of chymase-digested C-terminally truncated apolipoprotein A-I in normal human serum. *J. Immunol. Methods.* **369:** 51–58.
20. Tan, Y., T. R. Liu, S. W. Hu, D. Tian, C. Li, J. K. Zhong, H. G. Sun, T. T. Luo, W. Y. Lai, and Z. G. Guo. 2014. Acute coronary syndrome remodels the protein cargo and functions of high-density lipoprotein subfractions. *PLoS One.* **9:** e94264.
21. Gowri, M. S., D. R. Van der Westhuyzen, S. R. Bridges, and J. W. Anderson. 1999. Decreased protection by HDL from poorly controlled type 2 diabetic subjects against LDL oxidation may Be due to the abnormal composition of HDL. *Arterioscler. Thromb. Vasc. Biol.* **19:** 2226–2233.
22. Cubedo, J., T. Padro, X. Garcia-Moll, X. Pinto, J. Cinca, and L. Badimon. 2011. Proteomic signature of Apolipoprotein J in the early phase of new-onset myocardial infarction. *J. Proteome Res.* **10:** 211–220.
23. Cubedo, J., T. Padro, and L. Badimon. 2014. Glycoproteome of human apolipoprotein A-I: N- and O-glycosylated forms are increased in patients with acute myocardial infarction. *Transl. Res.* **164:** 209–222.
24. Garber, D. W., K. R. Kulkarni, and G. M. Anantharamaiah. 2000. A sensitive and convenient method for lipoprotein profile analysis of individual mouse plasma samples. *J. Lipid Res.* **41:** 1020–1026.
25. Karlsson, H., P. Leanderson, C. Tagesson, and M. Lindahl. 2005. Lipoproteomics I: mapping of proteins in low-density lipoprotein using two-dimensional gel electrophoresis and mass spectrometry. *Proteomics.* **5:** 551–565.
26. Cal, R., O. Juan-Babot, V. Brossa, S. Roura, C. Galvez-Monton, M. Portoles, M. Rivera, J. Cinca, L. Badimon, and V. Llorente-Cortes. 2012. Low density lipoprotein receptor-related protein 1 expression correlates with cholesteryl ester accumulation in the myocardium of ischemic cardiomyopathy patients. *J. Transl. Med.* **10:** 160.
27. Folch, J., M. Lees, and G. H. Sloane Stanley. 1957. A simple method for the isolation and purification of total lipides from animal tissues. *J. Biol. Chem.* **226:** 497–509.
28. Johnson, D. W., M. U. Trinh, and T. Oe. 2003. Measurement of plasma pristanic, phytanic and very long chain fatty acids by liquid chromatography-electrospray tandem mass spectrometry for the diagnosis of peroxisomal disorders. *J. Chromatogr. B Analyt. Technol. Biomed. Life Sci.* **798:** 159–162.
29. Sysi-Aho, M., M. Katajamaa, L. Yetukuri, and M. Oresic. 2007. Normalization method for metabolomics data using optimal selection of multiple internal standards. *BMC Bioinformatics.* **8:** 93.
30. Jaleel, A., G. C. Henderson, B. J. Madden, K. A. Klaus, D. M. Morse, S. Gopala, and K. S. Nair. 2010. Identification of de novo synthesized and relatively older proteins: accelerated oxidative damage to de novo synthesized apolipoprotein A-1 in type 1 diabetes. *Diabetes.* **59:** 2366–2374.
31. Rawlings, N. D., A. J. Barrett, and A. Bateman. 2012. MEROPS: the database of proteolytic enzymes, their substrates and inhibitors. *Nucleic Acids Res.* **40:** D343–D350.
32. Beg, Z. H., J. A. Stonik, J. M. Hoeg, S. J. Demosky, Jr., T. Fairwell, and H. B. Brewer, Jr. 1989. Human apolipoprotein A-I. Post-translational modification by covalent phosphorylation. *J. Biol. Chem.* **264:** 6913–6921.
33. Hoeg, J. M., M. S. Meng, R. Ronan, T. Fairwell, and H. B. Brewer, Jr. 1986. Human apolipoprotein A-I. Post-translational modification by fatty acid acylation. *J. Biol. Chem.* **261:** 3911–3914.
34. Fernández-Irigoyen, J., E. Santamaria, L. Sesma, J. Munoz, J. I. Riezu, J. Caballeria, S. C. Lu, J. Prieto, J. M. Mato, M. A. Avila, et al. 2005. Oxidation of specific methionine and tryptophan residues of apolipoprotein A-I in hepatocarcinogenesis. *Proteomics.* **5:** 4964–4972.
35. Nobecourt, E., M. J. Davies, B. E. Brown, L. K. Curtiss, D. J. Bonnet, F. Charlton, A. S. Januszewski, A. J. Jenkins, P. J. Barter, and K. A. Rye. 2007. The impact of glycation on apolipoprotein A-I structure and its ability to activate lecithin:cholesterol acyltransferase. *Diabetologia.* **50:** 643–653.

36. Che, W., M. Asahi, M. Takahashi, H. Kaneto, A. Okado, S. Higashiyama, and N. Taniguchi. 1997. Selective induction of heparin-binding epidermal growth factor-like growth factor by methylglyoxal and 3-deoxyglucosone in rat aortic smooth muscle cells. The involvement of reactive oxygen species formation and a possible implication for atherogenesis in diabetes. *J. Biol. Chem.* **272:** 18453–18459.
37. Eberini, I., L. Calabresi, R. Wait, G. Tedeschi, A. Pirillo, L. Puglisi, C. R. Sirtori, and E. Gianazza. 2002. Macrophage metalloproteinases degrade high-density-lipoprotein-associated apolipoprotein A-I at both the N- and C-termini. *Biochem. J.* **362:** 627–634.
38. Rogers, D. P., C. G. Brouillette, J. A. Engler, S. W. Tendian, L. Roberts, V. K. Mishra, G. M. Anantharamaiah, S. Lund-Katz, M. C. Phillips, and M. J. Ray. 1997. Truncation of the amino terminus of human apolipoprotein A-I substantially alters only the lipid-free conformation. *Biochemistry.* **36:** 288–300.
39. Fang, Y., O. Gursky, and D. Atkinson. 2003. Lipid-binding studies of human apolipoprotein A-I and its terminally truncated mutants. *Biochemistry.* **42:** 13260–13268.
40. Li, L., J. Chen, V. K. Mishra, J. A. Kurtz, D. Cao, A. E. Klon, S. C. Harvey, G. M. Anantharamaiah, and J. P. Segrest. 2004. Double belt structure of discoidal high density lipoproteins: molecular basis for size heterogeneity. *J. Mol. Biol.* **343:** 1293–1311.
41. Gu, F., M. K. Jones, J. Chen, J. C. Patterson, A. Catte, W. G. Jerome, L. Li, and J. P. Segrest. 2010. Structures of discoidal high density lipoproteins: a combined computational-experimental approach. *J. Biol. Chem.* **285:** 4652–4665.
42. Sasongko, M. B., T. Y. Wong, T. T. Nguyen, R. Kawasaki, A. Jenkins, J. Shaw, and J. J. Wang. 2011. Serum apolipoprotein AI and B are stronger biomarkers of diabetic retinopathy than traditional lipids. *Diabetes Care.* **34:** 474–479.
43. Feron, D., A. Begu-Le Corroller, J. M. Piot, C. Frelicot, B. Vialettes, and I. Fruitier-Arnaudin. 2009. Significant lower VVH7-like immunoreactivity serum level in diabetic patients: evidence for independence from metabolic control and three key enzymes in hemorphin metabolism, cathepsin D, ACE and DPP-IV. *Peptides.* **30:** 256–261.
44. Usami, Y., Y. Kobayashi, T. Kameda, A. Miyazaki, K. Matsuda, M. Sugano, K. Kawasaki, Y. Kurihara, T. Kasama, and M. Tozuka. 2013. Identification of sites in apolipoprotein A-I susceptible to chymase and carboxypeptidase A digestion. *Biosci. Rep.* **33:** 49–56.
45. Hakala, J. K., R. Oksjoki, P. Laine, H. Du, G. A. Grabowski, P. T. Kovanen, and M. O. Pentikainen. 2003. Lysosomal enzymes are released from cultured human macrophages, hydrolyze LDL in vitro, and are present extracellularly in human atherosclerotic lesions. *Arterioscler. Thromb. Vasc. Biol.* **23:** 1430–1436.
46. Vivanco, F., J. L. Martin-Ventura, M. C. Duran, M. G. Barderas, L. Blanco-Colio, V. M. Darde, S. Mas, O. Meilhac, J. B. Michel, J. Tunon, et al. 2005. Quest for novel cardiovascular biomarkers by proteomic analysis. *J. Proteome Res.* **4:** 1181–1191.
47. Scheffer, P. G., T. Teerlink, and R. J. Heine. 2005. Clinical significance of the physicochemical properties of LDL in type 2 diabetes. *Diabetologia.* **48:** 808–816.
48. Mora, S., J. D. Otvos, R. S. Rosenson, A. Pradhan, J. E. Buring, and P. M. Ridker. 2010. Lipoprotein particle size and concentration by nuclear magnetic resonance and incident type 2 diabetes in women. *Diabetes.* **59:** 1153–1160.
49. Vakkilainen, J., G. Steiner, J. C. Ansquer, F. Aubin, S. Rattier, C. Foucher, A. Hamsten, and M. R. Taskinen. 2003. Relationships between low-density lipoprotein particle size, plasma lipoproteins, and progression of coronary artery disease: the Diabetes Atherosclerosis Intervention Study (DAIS). *Circulation.* **107:** 1733–1737.
50. Guérin, M., W. Le Goff, T. S. Lassel, A. Van Tol, G. Steiner, and M. J. Chapman. 2001. Atherogenic role of elevated CE transfer from HDL to VLDL(1) and dense LDL in type 2 diabetes: impact of the degree of triglyceridemia. *Arterioscler. Thromb. Vasc. Biol.* **21:** 282–288.
51. Llorente-Cortés, V., M. Otero-Vinas, E. Hurt-Camejo, J. Martinez-Gonzalez, and L. Badimon. 2002. Human coronary smooth muscle cells internalize versican-modified LDL through LDL receptor-related protein and LDL receptors. *Arterioscler. Thromb. Vasc. Biol.* **22:** 387–393.
52. Rohrer, L., M. Hersberger, and A. von Eckardstein. 2004. High density lipoproteins in the intersection of diabetes mellitus, inflammation and cardiovascular disease. *Curr. Opin. Lipidol.* **15:** 269–278.
53. Kougias, P., H. Chai, P. H. Lin, A. B. Lumsden, Q. Yao, and C. Chen. 2006. Lysophosphatidylcholine and secretory phospholipase A2 in vascular disease: mediators of endothelial dysfunction and atherosclerosis. *Med. Sci. Monit.* **12:** RA5–RA16.
54. Davidsson, P., J. Hulthe, B. Fagerberg, B. M. Olsson, C. Hallberg, B. Dahllof, and G. Camejo. 2005. A proteomic study of the apolipoproteins in LDL subclasses in patients with the metabolic syndrome and type 2 diabetes. *J. Lipid Res.* **46:** 1999–2006.
55. Jang, W., N. H. Jeoung, and K. H. Cho. 2011. Modified apolipoprotein (apo) A-I by artificial sweetener causes severe premature cellular senescence and atherosclerosis with impairment of functional and structural properties of apoA-I in lipid-free and lipid-bound state. *Mol. Cells.* **31:** 461–470.